

Simple Cubic Carbon Phase C21-sc: A Promising Superhard Carbon Conductor

Chaoyu He,^{1,2} Lijun Meng,^{1,2} Chao Tang,^{1,2} and Jianxin Zhong^{1,2,*}

¹Hunan Key Laboratory for Micro-Nano Energy Materials and Devices, Xiangtan University, Hunan 411105, P. R. China;

²School of Physics and Optoelectronics, Xiangtan University, Xiangtan 411105, China.

(Dated: June 27, 2021)

Traditionally, all superhard carbon phases including diamond are electric insulators and all conductive carbon phases including graphite are mechanically soft. Based on first-principles calculation results, we report a superhard but conductive carbon phase C21-sc which can be obtained through increasing the sp^3 bonds in the previously proposed soft and conductive phase C20-sc (**Phys. Rev. B** **74**, 172101 2006). We also show that further increase of sp^3 bonds in C21-sc results in a superhard and insulating phase C22-sc with sp^3 bonds only. With C20-sc, C21-sc, C22-sc and graphite, the X-ray diffraction peaks from the unidentified carbon material synthesized by compressing the mixture of tetracyanoethylene and carbon black (**Carbon**, **41**, 1309, 2003) can be understood. In view of its positive stability, superhard and conductive features, and the strong possibility of existence in previous experiments, C21-sc is a promising multi-functional material with potential applications in extreme conditions.

PACS numbers: 61.66.Bi, 62.20.D-, 63.20.D-, 71.15.Mb

Superhard materials with extreme Vicker's hardness larger than 40 GPa are widely used in mechanical industry. For instance, diamond and cubic boron nitride with extreme hardness are often used as tools for cutting and polishing other materials. However, both diamond and cubic boron nitride are electronic insulating. Most of other superhard materials are also electronic insulating. In the past decade, many efforts have been paid on searching for superhard and conductive materials¹⁻⁵ for multi-functional applications in extreme conditions. For example, the boron-doped diamond^{1,5} can be superhard and conductive due to its diamond structure for superhard mechanical property and the addition of the necessary electrons for conductivity from boron.

Carbon with broad sp , sp^2 and sp^3 hybridizing ability can form numerous carbon allotropes, including the superhard diamond and the very soft graphite. Superhard carbon phases (diamond and its allotropes) are optically transparent insulators and conductive carbon phases (graphite and its allotropes) are mechanically soft. The superhardness of diamond and its allotropes is mainly contributed by the entire covalent sp^3 short bonds, which result in insulating electronic properties. Based on numerous previous investigations on the mechanical and electronic properties of different carbon allotropes, one may conclude that carbon allotropes with entire sp^3 hybridization⁶⁻¹² are always mechanically superhard and electronically insulating. Carbon allotropes with entire sp^2 hybridization¹³⁻¹⁸ are always mechanically soft, but they are not always metallic. For example, one has soft and metallic bct-4¹³, C20¹⁷ and H6-carbon^{14,15}, as well as soft and insulating polybenzene¹⁶ and sp^2 -diamond¹⁸. All the previously proposed carbon phases with mixed sp^2 and sp^3 bonds¹⁹⁻²³ are soft materials which can be metals or insulators. There is no carbon phase with both superhard and conductive features in the published literature. In this letter, we report a simple cubic carbon phase C21-sc which is superhard and conductive. C21-sc can be constructed by increasing the sp^3 bonds in the previously proposed metallic carbon phase C20-sc²³ with both sp^2 and sp^3 bonds. Further

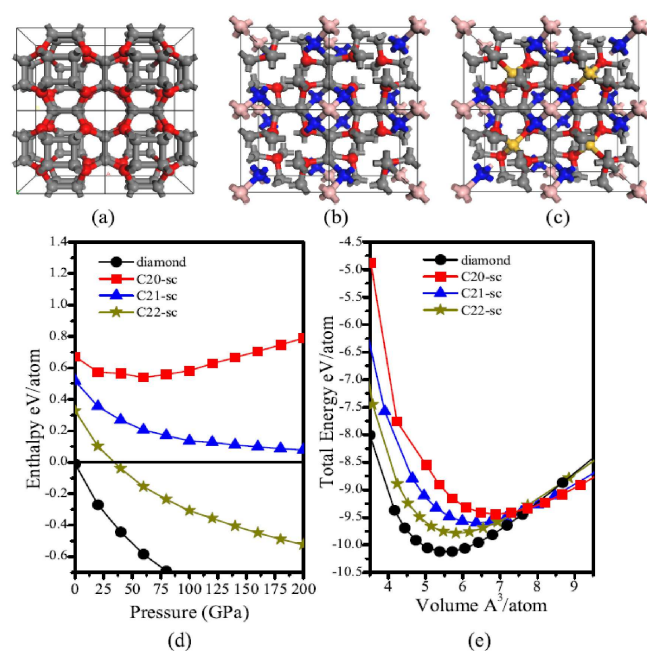


FIG. 1: Perspective view of C20-sc (a), C21-sc (b) and C22-sc (c) in their crystalline cells. Balls in different colors indicate different atoms (Their positions 1, 2, 3, 4 and 5 listed in Table I are correspondingly marked in red, blue, grey, brown and yellow, respectively.); E-P cures (d) of diamond, C20-sc, C21-sc and C22-sc relative to graphite and E-V cures (e) of diamond, C20-sc, C21-sc and C22-sc.

increase of sp^3 bonds in C21-sc results in a superhard but insulating phase C22-sc with sp^3 bonds only. We show that with C20-sc, C21-sc, C22-sc and graphite, the X-ray diffraction peaks found in an unidentified carbon material²⁴ can be understood.

All calculations of structural optimization and properties are carried out using the density functional theory within

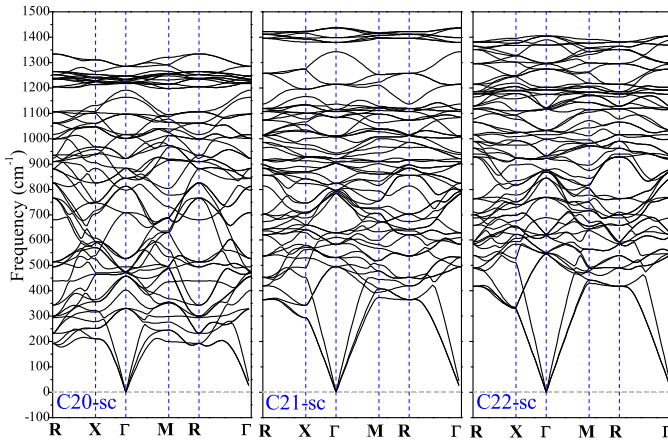


FIG. 2: Phonon band structures of C20-sc, C21-sc and C22-sc.

local density approximation (LDA)^{25,26} as implemented in Vienna ab initio simulation package (VASP)^{27,28}. The interactions between nucleus and the $2s^2 2p^2$ valence electrons of carbon are described by the projector augmented wave (PAW) method^{29,30}. A plane-wave basis with a cutoff energy of 500 eV is used to expand the wave functions and the Brillouin Zone (BZ) sample meshes are set to be dense enough (less than 0.21 \AA^{-1}) to ensure the accuracy of calculations. The structures of C20-sc, C21-sc, C22-sc and diamond are fully optimized up to the residual force on every atom less than 0.005 eV/\AA . The vibrational properties of C20-sc, C21-sc and C22-sc are investigated by using the PHONON package³¹ with the forces calculated from VASP to evaluate their dynamical stability. The three inequivalent elastic constants (C_{11} , C_{12} and C_{44}) of diamond, C20-sc, C21-sc and C22-sc are calculated as the second-order coefficients in the polynomial function of distortion parameter δ used to fit their total energies according to the Hooke's law. Three groups of deformations, namely, ($e_{1,2}=\delta$, $e_3=(1+\delta)^{-2}-1$, $e_{4,5,6}=0$), ($e_{1,2,3}=\delta$, $e_{4,5,6}=0$), and ($e_6=\delta$, $e_3=\delta^2(4-\delta^2)^{-1}$, $e_{1,2,5}=0$) are considered in each cubic phase. The bulk modulus (\mathbf{B}) and shear modulus (\mathbf{G}) are evaluated according to Hill's formula³² based on the calculated elastic constants. To further analyze the hardness of these carbon allotropes, we adopt the recently introduced empirical scheme³³ to evaluate Vicker's hardness (H_v) determined by \mathbf{B} and \mathbf{G} as $H_v=2(\mathbf{G}^3/\mathbf{B}^2)^{0.585}-3$.

C20-sc contains 20 carbon atoms in its cubic cell (Pm-3m) with lattice constant of 5.163 \AA . It has two inequivalent carbon atoms, namely, sp^2 and sp^3 carbon atoms locating at positions of $8g$ ($0.238, 0.238, 0.238$) and $12i$ ($0.00, 0.651, 0.651$), respectively. The eight sp^2 carbon atoms symmetrically distribute on the body diagonal of the cubic cell, which role as inter-linkers between the surface squares formed by the sp^3 carbon atoms. There are two inequivalent carbon bonds in C20-sc, namely, the inner-square ones B_{33} containing only sp^3 carbon atoms (we mark bonds as B_{ij} and angles as θ_{ijk} , where i, j and k mean different types of carbon atoms as indicated in Table I.) and the inter-square ones B_{13} linking the sp^2 and sp^3 carbon atoms. The corresponding bond lengths are $B_{33}=1.564 \text{ \AA}$ and $B_{13}=1.471 \text{ \AA}$, which are

close to those in diamond and graphite, respectively. The four distinct bond angles in C20-sc are $\theta_{333}=90^\circ$, $\theta_{331}=112.95^\circ$, $\theta_{131}=113.06^\circ$ and $\theta_{313}=120^\circ$, respectively.

With standard sp^2 hybridization and distorted sp^3 hybridization, C20-sc possesses relatively high energy. Its cohesive energy of -8.315 eV/atom is 674 meV higher than that of diamond. However, C20-sc is more favorable than the experimentally viable graphdiyne. Its cohesive energy is about 300 meV per atom lower than that of graphdiyne (-8.083 eV/atom), indicating that it is experimentally viable too. Moreover, our calculations on its vibrational property show that there is no imaginary frequency in its phonon band structure (see in Fig.2), which confirms that C20-sc is a dynamically stable. Its calculated elastic constants (see Tab I) also satisfy the mechanical stability criteria of cubic lattice, suggesting that C20-sc is mechanically stable too. The phase stability of C20-sc can also be confirmed by the quadratic E-V relation near the equilibrium V_0 as shown in Fig.1 (e).

As a cage-like structure with the ratio of 2:3 for sp^2 and sp^3 bonds, C20-sc is a sparse, soft and conductive material. From Fig.1 (e), we can see that C20-sc possesses a relatively larger equilibrium volume (V_0). Its mass density of 2.899 Mg/cm^3 is just a little higher than that of graphite and its verker's hardness is very low (17.79 GPa) in comparison with that of diamond. From the calculated electronic band structures (EBS) and projected energy density of states (PDOS) of C20-sc (see Fig.3), we can see that C20-sc is a metallic phase with states around and crossing the Fermi-level. The PDOS shows that the metallic states around the Fermi-level in C20-sc are mainly contributed from the sp^2 hybridized carbon atoms. While the sp^3 hybridized carbon atoms contribute states locating at relatively lower energy area. From the bonding charge density of C20-sc shown in Fig.3, we can see that bonding charge in C20-sc distribute around sp^3 and sp^2 carbon atoms with tetrahedral and triangular patterns, respectively.

Based on the relation between the structure and electronic property of C20-sc as well as the common knowledge that more sp^3 hybridization leads to higher hardness, we modify the structure of C20-sc to construct the new carbon phase C21-sc which can be superhard and conductive. As shown in Fig.1, we construct C21-sc through adding carbon atoms (colored in brown) in C20-sc at the vertex positions of $1a$ ($0.000, 0.000, 0.000$) and moving 4 of the 8 sp^2 carbon atoms (colored in blue), from $4e$ ($0.238, 0.238, 0.238$) to $4e$ ($0.176, 0.176, 0.176$) along the body diagonal toward to the vertex to enclose the added vertex atoms in standard tetrahedrons with proper size, for standard sp^3 hybridization. Such an operation reduces the symmetry of the system from Pm-3m to F-43m and changes C20-sc to C21-sc with reduced sp^2 carbon atoms (with the ratio of 4:17 for $sp^2:sp^3$). After optimization, the lattice constant of C21-sc is 5.112 \AA . From table I, we can see that with the added atoms at $1a$ position, the atoms at $8g$ position in C20-sc decompose into two inequivalent groups locating at two inequivalent positions of $4e$ ($0.278, 0.278, 0.278$) and $4e$ ($0.176, 0.176, 0.176$) with sp^2 and sp^3 hybridizations, respectively. It should be noticed that carbon atoms at the sp^2 positions slightly move toward the

TABLE I: Fundamental structural information, cohesive energies, elastic constants and mechanical properties of diamond, C20-sc, C21-sc and C22-sc.

Items	Diamond	C20-sc	C21-sc	C22-sc
Space group	Fd-3m (No.227)	Pm-3m (No.221)	P-43m (No.215)	P-43m (No.215)
Lattice constant	3.536 Å	5.163 Å	5.112 Å	5.097 Å
Mass density	3.611 Mg/cm ³	2.899 Mg/cm ³	3.134 Mg/cm ³	3.313 Mg/cm ³
Cohesive energy	-8.989	-8.315	-8.471	-8.661
Position 1 (red)	8a:0.000,0.000,0.000	8g:0.238,0.238,0.238	4e:0.278,0.278,0.278	4e:0.304,0.304,0.304
Position 2 (blue)	-	-	4e:0.176,0.826,0.176	4e:0.176,0.826,0.176
Position 3 (grey)	-	12i:0.00, 0.651,0.349	12i:0.000,0.651,0.349	12i:0.981,0.649,0.351
Position 4 (brown)	-	-	1a:0.000,0.000,0.000	1a:0.000,0.000,0.000
Position 5 (yellow)	-	-	-	1b:0.500,0.500,0.500
C ₁₁	1100.46 GPa	577.13 GPa	754.73 GPa	959.79 GPa
C ₁₂	149.73 GPa	275.89 GPa	168.61 GPa	99.46 GPa
C ₄₄	589.91 GPa	243.89 GPa	370.99 GPa	453.97 GPa
Shear modulus	541.07 GPa	195.55 GPa	337.57 GPa	444.29 GPa
Bulk modulus	466.64 GPa	369.64 GPa	363.98 GPa	386.24 GPa
Verker's hardness	91.44 GPa	17.79 GPa	52.19 GPa	80.38 GPa

vertex (from (0.238, 0.238, 0.238) in C20-sc to (0.278, 0.278, 0.278) in C21-sc) after optimization, forming a non-planar sp² configuration. The sp³ carbon atoms still locate at the 12i position of (0.000, 0.651, 0.349).

There are four distinct C-C bonds in C21-sc which are B₃₃=1.540 Å, B₁₃=1.431 Å, B₂₃=1.602 Å and B₂₄=1.562 Å. Three equivalent bond angles around atom 1 are formed by the triangularly distributed atoms 3. They are sp²-like bond angles of 114.5° (θ_{313}), which is slightly smaller than that of the standard sp² hybridization (120°). Two inequivalent bond angles around atom 2 are θ_{323} and θ_{324} of 112.29° and 106.48°, respectively. The four inequivalent bond angles around atom 3 are θ_{333} =89.26°, θ_{133} =111.46°, θ_{233} =118.62° and θ_{132} =106.79°. Four equivalent atoms 2 tetrahedrally distribute around atom 4, forming six equivalent sp³ hybridized bond angles θ_{242} of 109.47°.

With the increased sp³ hybridization, C21-sc is energetically more favorable than C20-sc. Its cohesive energy of -8.471 eV/atom is about 160 meV lower than that of C20-sc. As shown in Fig.1 (d), its energetic stability gradually approaches to that of graphite as the external pressure increases. Fig.2 shows the phonon band structure of C21-sc, which confirms the positive dynamical stability of C21-sc. The three independent elastic constants of C21-sc with C₁₁=754.73 GPa, C₁₂=168.61 GPa and C₄₄=370.99 GPa satisfy the mechanical stability criteria, indicating that C21-sc is mechanically stable too. In Fig.1 (e), the phase stability of C21-sc is also confirmed by the quadratic E-V relation near the equilibrium V₀.

C21-sc still contains 4 sp² hybridized carbon atoms per cubic cell. Its mass density of 3.134 Mg/cm³ is just a little higher than that of C20-sc. As expected, the increased sp³ ratio makes C21-sc harder than C20-sc. In fact, C21-sc is a superhard material in view of its high verker's hardness of 52.19 GPa. It is exciting that C21-sc is electrically conductive. From the calculated EBS and PDOS of C21-sc, we can see that the reduction of sp² hybridized carbon atoms reduces the numbers of the energy bands around Fermi-level. However, C21-sc still behaves as a classical metal with obvious

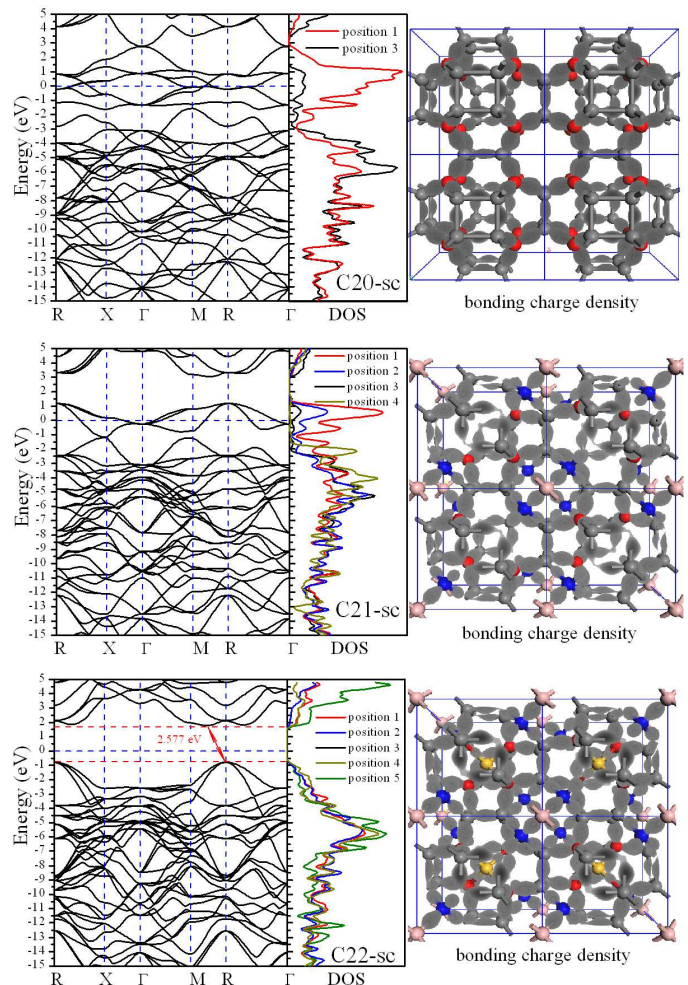


FIG. 3: Electronic band structures (left), projected energy density of states (middle) and bonding charge density (right) of C20-sc (top), C21-sc (center) and C22-sc (bottom).

electronic bands crossing the Fermi-level. From the PDOS shown in Fig.3, the metallic states around the Fermi-level are mainly contributed by the sp^2 hybridized atoms 1. We can also see that the bonding charge density (Fig.3) distributes on the sp^3 atoms with tetrahedral configurations and on the sp^2 atoms with triangular configurations.

Further modification of C20-sc by adding carbon atoms (colored in yellow) at the body center 1b (0.500, 0.500, 0.500) in C21-sc provides us a new superhard insulating phase C22-sc. Detailed structural information of C22-sc is given in Tab I. After optimization, the lattice constant of C22-sc is reduced, in comparison with that of C21-sc, to 5.097 Å. With the entirely sp^3 hybridization, C22-sc is energetically more favorable than C20-sc and C21-sc. Its cohesive energy of -8.661 eV/atom is about 180 meV lower than that of C21-sc. Specially, C22-sc becomes more stable than graphite when the external pressure increases to 34 GPa, which is in good agreement with the fact that high pressure prefers saturated bonds than unsaturated ones³⁴⁻³⁶. Both the dynamical and mechanical stabilities of C22-sc are confirmed to be positive by its phonon band structure and elastic constants, respectively.

With sp^3 carbon atoms only, C22-sc becomes denser and harder than C20-sc and C21-sc. Its mass density of 3.313 Mg/cm³ is slightly smaller than that of diamond and its verker's hardness of 80.38 GPa is comparable to that of diamond. The whole sp^3 hybridization makes C22-sc an insulator. As shown in Fig.3, it possesses an indirect band gap of 2.577 eV. The bonding charge density in C22-sc tetrahedrally distributes on the sp^3 bonds around every carbon atom.

The above theoretical results show that C21-sc possesses both superhard and conductive properties, which can be potentially used as a multi-functional material in extreme conditions. In fact, in a previous experimental work in 2003²⁴, a pure carbon material was synthesized by compressing the mixture of tetracyanoethylene and carbon black. The new carbon material possesses a simple cubic lattice with lattice constant of 5.14 Å, which is very close to those of C20-sc, C21-sc and C22-sc. In the experimental work, it is believed that six X-ray diffraction peaks (B1-B6 marked as red solid circles) are contributed from graphite, while nine new peaks (marked as A1-A9 with black solid triangles in Fig.4) are contributed by an unknown new carbon phase. After simulation of the X-ray diffraction of C20-sc, C21-sc and C22-sc, we find that the experimental X-ray diffraction peaks can be understood by the contribution of graphite, C20-sc, C21-sc and C22-sc. As shown in Fig.4, we believe that peaks A1, A2 and A4 are from C20-sc, A3 from graphite, A7 from C22-sc and A9 from C21-sc. From our understanding, peaks B1-B6 are not from graphite. Although the position of B1 corresponds to graphite, its width can not be understood solely with graphite. We find that the existence of C20-sc and C21-sc can well explain the width of peak B1 and it is better to explain B3 with C22-sc, B4 and B5 with C20-sc and B6 with C21-sc rather than graphite. Especially, we find that all the X-ray diffraction peaks of graphite, C20-sc,

C21-sc and C22-sc can be used to explain other peaks found

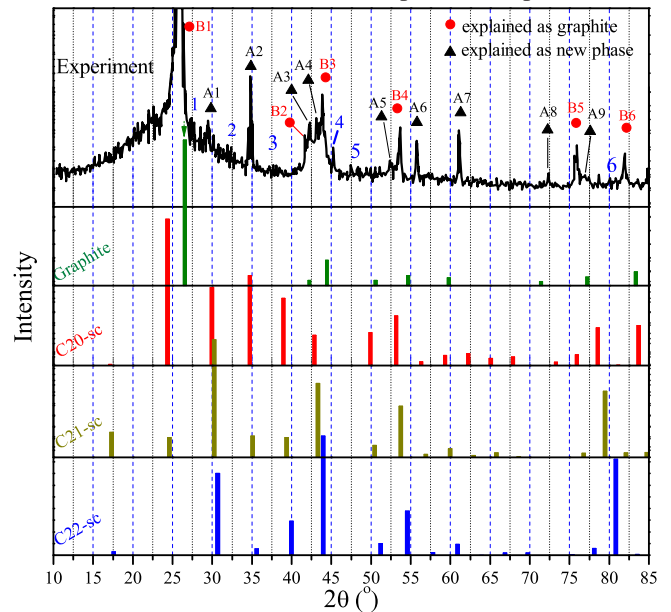


FIG. 4: Experimental X-ray diffraction patterns of the new carbon material²⁴(black lines) and simulated X-ray diffraction peaks of graphite (green), C20-sc (red), C21-sc (dark yellow) and C22-sc (blue).

in the experiment. The excellent match of lattice constants and X-ray diffraction peaks suggest the synthesized material contain graphite, C20-sc, C21-sc and C22-sc.

In summary, through modification of the soft and conductive carbon phase C20-sc, we have predicted two new cubic carbon phases C21-sc and C22-sc which possess viable energetic stability, positive dynamical and mechanical stabilities. Both C21-sc and C22-sc are superhard materials similar to diamond. However, C21-sc is electrically conductive while C22-sc is insulating. We show that the X-ray diffraction peaks in an unknown cubic carbon material synthesized by compressing a mixture of tetracyanoethylene and carbon black can be understood from the characteristic diffraction peaks of C20-sc, C21-sc, C22-sc and graphite. The strong theoretical and experimental evidences of the existence of superhard and conductive carbon C21-sc may open a new window for the study of multi-functional materials in extreme conditions.

This work is supported by the National Natural Science Foundation of China (Grant Nos. A040204 and 11204261), the National Basic Research Program of China (2012CB921303 and 2015CB921103), the Hunan Provincial Innovation Foundation for Postgraduate (Grant No. CX2013A010), the Young Scientists Fund of the National Natural Science Foundation of China (Grant No. 11204260), and the Program for Changjiang Scholars and Innovative Research Team in University (IRT13093).

- * Electronic address: jxzhong@xtu.edu.cn
- ¹ Z. Y. Liu, J. L. He, J. Yang, X. J. Guo, H. Sun, H. T. Wang, E. Wu and Y. J. Tian, *Phys. Rev. B*, **73**, 172101 (2006).
 - ² V. L. Solozhenko, O. O. Kurakevych, D. Andrault, Y. Le Codec and M. Mezouar, *Phys. Rev. Lett.* **102**, 015506 (2009).
 - ³ H. B. Wang, Q. Li, H. Wang, H. Y. Liu, T. Cui and Y. M. Ma, *J. Phys. Chem. C*, **114**, 8609 (2010).
 - ⁴ J. Yang, H. Sun, J. L. He, Y. J. Tian and C. F. Chen, *J. Phys.: Condens. Matter* **19**, 346223 (2007).
 - ⁵ L. F. Xu, Z. S. Zhao, L. M. Wang, B. Xu, J. L. He, Z. Y. Liu and Y. J. Tian, *J. Phys. Chem. C* **114**, 22688 (2010).
 - ⁶ Q. Li, Y. M. Ma, A. R. Oganov, H. B. Wang, H. Wang, Y. Xu, T. Cui, H. K. Mao, and G. T. Zou, *Phys. Rev. Lett.* **102**, 175506 (2009).
 - ⁷ J. T. Wang, C. F. Chen and Y. Kawazoe, *Phys. Rev. Lett.* **106**, 075501 (2011).
 - ⁸ Z. S. Zhao, B. Xu, X. F. Zhou, L. M. Wang, B. Wen, J. L. He, Z. Y. Liu, H. T. Wang and Y. J. Tian, *Phys. Rev. Lett.* **107**, 215502 (2011).
 - ⁹ C. Y. He, L. Z. Sun, C. X. Zhang, X. Y. Peng, K. W. Zhang and J. X. Zhong, *Phys. Chem. Chem. Phys.* **14**, 8410 (2012).
 - ¹⁰ C. Y. He, L. Z. Sun, and J. X. Zhong, *J. Superhard Mater.* **34**, 386 (2012).
 - ¹¹ C. Y. He, L. Z. Sun, C. X. Zhang, X. Y. Peng, K. W. Zhang, and J. X. Zhong, *Solid state commun.* **152**, 1560 (2012).
 - ¹² Q. Zhu, Q. Zeng and A. R. Oganov, *Phys. Rev. B* **85**, 201407 (2012).
 - ¹³ R. Hoffmann, T. Hughbanks and K. Kertész, *J. Am. Chem. Soc.* **105**, 4831 (1983).
 - ¹⁴ M. A. Tamor and K. C. Hass, *J. Mater. Res.*, **5**, 2273 (1990).
 - ¹⁵ A. Y. Liu, M. L. Cohen, M. A. Tamor and K. C. Hass, *Phys. Rev. B* **43**, 6742 (1990).
 - ¹⁶ M. O'Keeffe, G. B. Adams and O. F. Sankey, *Phys. Rev. Lett.* **68**, 2325 (1992).
 - ¹⁷ M. Côté, J. C. Grossman, M. L. Cohen, S. G. Louie, *Phys. Rev. B* **58**, 664 (1998).
 - ¹⁸ C. Y. He, L. Z. Sun, C. X. Zhang and J. X. Zhong, *J. X.*, *Phys. Chem. Phys. Chem.* **15**, 680 (2013).
 - ¹⁹ F. J. Ribeiro, P. Tangney, S. G. Louie, and M. L. Cohen, *Phys. Rev. B*, **72**, 214109 (2005).
 - ²⁰ K. Agnieszka and S. Gotthard, *Phys. Rev. B* **74**, 214104 (2006).
 - ²¹ M. Hu, Z. S. Zhao, F. Tian, A. R. Oganov, Q. Q. Wang, M. Xiong, C. Z. Fan, B. Wen, J. L. He, D. L. Yu, H. T. Wang, B. Xu, and Y. J. Tian, *Sci. Rep.* **3**, 1331 (2013).
 - ²² X. Jiang, J. J. Zhao, Y. L. Li and R. Ahuja, *Adv. Funct. Mater.* **23**, 5846 (2013).
 - ²³ F. Ribeiro, P. Tangney, S. Louie, and M. Cohen, *Phys. Rev. B* **74**, 172101 (2006).
 - ²⁴ K. Yamada, *Carbon*, **41**, 1309 (2003).
 - ²⁵ D. M. Ceperley and B. J. Alder, *Phys. Rev. Lett.* **45**, 566 (1980).
 - ²⁶ J. P. Perdew and A. Zunger, *Phys. Rev. B* **23**, 5048 (1981).
 - ²⁷ G. Kresse and J. Furthmüller, *Phys. Rev. B* **54**, 11169 (1996).
 - ²⁸ G. Kresse and J. Furthmüller, *Comput. Mater. Sci.* **6**, 15 (1996).
 - ²⁹ P. E. Blöchl, *Phys. Rev. B* **50**, 17953 (1994).
 - ³⁰ G. Kresse and D. Joubert, *Phys. Rev. B* **59**, 1758 (1999).
 - ³¹ K. Parlinski, Z.-Q. Li, and Y. Kawazoe, *Phys. Rev. Lett.* **78**, 4063 (1997).
 - ³² R. Hill, *Proc. Phys. Soc. A* **65**, 349 (1952).
 - ³³ H. Y. Niu, P. Y. Wei, Y. Sun, X. Q. Chen, C. Franchini, D. Z. Li, Y. Y. Li, *Appl. Phys. Lett.* **99**, 031901 (2011).
 - ³⁴ W. L. Mao, H. Mao, P. J. Eng, T. P. Trainor, M. Newville, C. C. Kao, D. L. Heinz, J. F. Shu, Y. Eng and R. J. Hemley, *Science* **302**, 425 (2003).
 - ³⁵ X. D. Wen, R. Hoffmann, and N. W. Ashcroft, *J. Am. Chem. Soc.* **133**, 9023 (2011).
 - ³⁶ C. Y. He, L. Z. Sun, C. X. Zhang, and J. X. Zhong, *J. Phys.:condens. Mater* **25**, 205403 (2013).